J Electr Eng Technol Vol. 8, No. 1: 150-155, 2013
http://dx.doi.org/10.5370/JEET.2013.8.1.150

ISSN(Print) 1975-0102
ISSN(Online) 2093-7423

Analysis of Output Pulse of High Voltage and Nanosecond Blumlein Pulse Generator

Young-Su Roh† and Yun-Sik Jin*

Abstract – A high voltage and nanosecond Blumlein pulse generator has been developed to produce an output pulse whose voltage level is greater than 250 kV and pulse duration 5 ns. The generator consists of various components such as a charging circuit, a pulse transformer, and a spark gap switch. As a heart of the generator, a Blumlein pulse forming line has been constructed in the cylindrical form using three cylindrical aluminum electrodes that are placed concentrically. Unlike the ideal Blumlein line, the output pulse of an actual Blumlein line may be affected by stray inductances and capacitances of switching and charging components, thereby degrading the performance of the generator. In this paper, PSPICE simulations have been performed to examine effects of stray inductances and capacitances on waveforms of output pulses. Simulation results show that the pulse waveform is significantly distorted mainly by the stray inductance of the spark gap switch.

Keywords: High voltage, Nanosecond, Pulse generator, Blumlein pulse forming line, PSPICE

1. Introduction

The Blumlein pulse forming line (PFL) is capable of generating a perfectly square voltage pulse, whose amplitude exactly equals that of the line charging voltage, to a matched load [1]. Moreover, it is straightforward to design the Blumlein PFL in terms of output impedance, pulse duration, and voltage by a suitable choice of the dimensions of the Blumlein conductor and the dielectric material serving as the energy storage medium [2, 3]. Due to such unique features, high voltage generators based on the Blumlein PFL have been widely used for research and development purposes in a variety of pulse power applications [4-8]. However, it is impossible to achieve a perfectly square voltage pulse in the operation of an actual Blumlein PFL because several spurious signals exist in the Blumlein line. Such signals may be caused by stray inductance and capacitance of switching and charging components.

The Blumlein PFL can be fabricated either in cylindrical form or in parallel plate configuration [3]. This paper presents a high voltage pulse generator based on a cylindrical type of Blumlein PFL. The primary objective of the pulse generator is to radiate extremely intense and fast transient electromagnetic waves for the examination of interactions between electromagnetic, ultra-wide band (UWB) pulses and electronic devices. The design goal of the Blumlein PFL is to produce an output voltage pulse whose amplitude is at a level of 250 kV and pulse duration is 5 ns. To obtain UWB electric fields, the rise time of the pulse must be as fast as possible.

For extremely high voltage switching of the Blumlein PFL, a gas pressurized spark gap switch is typically employed as the main switch to initiate the propagation of a step voltage along the Blumlein line. However, a stray inductance appears due to the spark channel created between two electrodes in the switch. This implies that the switch performance is determined by the stray inductance of the spark channel [9].

In the structure of the cylindrical Blumlein PFL, three cylindrical conductors, such as inner, middle, and outer conductors, are concentrically placed to construct the Blumlein line. As will be explained later, the high voltage output of a pulse transformer is applied to the middle conductor and the outer conductor is electrically grounded. A charging inductor is used to connect the inner conductor and the outer conductor. For a proper operation of the pulse generator, the charging inductor must act as a short circuit in the charging process of the Blumlein PFL, but it should play a role as an open circuit in the pulse forming process. Unfortunately, the inductor includes stray capacitances because of its closely spaced windings [10]. Such stray capacitance cannot be neglected at high frequencies and may affect the waveform of the Blumlein output pulse.

It was observed in the experiment that the waveform of the output pulse of the fabricated Blumlein PFL was significantly deformed. Especially, the rise time as well as the pulse duration was longer than the design value. In order to understand the experimental result and to find a method of improving the performance of the pulse generator, in this paper, the effects of the stray inductance of the spark gap switch on the Blumlein output pulse are examined in terms of pulse duration and rise time using PSPICE simulation. The stray capacitance of the charging

† Corresponding Author: Dept. of Electrical and Electronic Engineering, Soongsil University, Korea. (yroh@ssu.ac.kr)
* Electric Propulsion Research Division, Korea Electrotechnology Research Institute, Korea. (ysjin@keri.re.kr)
Received: December 16, 2012; Accepted: June 5, 2012

inductor is also included in the simulation model to investigate its effects on the output pulse.

The remainder of the paper is organized as follows. In Section 2, the operation principle of the Blumlein PFL is presented. In Section 3, a brief description of the high voltage and nanosecond pulse generator with detailed explanation on the Blumlein line. In Section 4, simulation results are provided and compared to experimental data. Finally, in Section 5, conclusion and future work are presented.

2. Operation Principle of Blumlein PFL

Fig. 1 shows the basic configuration of a single-stage Blumlein PFL based on the use of two coaxial and lossless transmission lines and a single switch. Here, the two transmission lines have identical properties in terms of characteristic impedance and length. The inductance per unit length (L) and the capacitance per unit length (C) of a coaxial transmission line with an inner conductor of radius R_i and an outer conductor of inner radius R_o can be expressed by

$$L = \frac{\mu_0 \mu_r}{2\pi} \ln \frac{R_o}{R_i} \text{ [H/m]}. \quad (1)$$

$$C = \frac{2\pi \varepsilon_0 \varepsilon_r}{\ln\left(R_o / R_i\right)} \text{ [F/m]}. \quad (2)$$

Here, μ_0 and ε_0 are the permeability and the permittivity of free space. μ_r and ε_r are the relative permeability and the relative permittivity of the medium between inner and outer conductors, respectively. Then, the characteristic impedance of the lossless transmission line is given by

$$Z_0 = \sqrt{\frac{L}{C}} = 60\sqrt{\frac{\mu_r}{\varepsilon_r}} \ln \frac{R_o}{R_i} [\Omega]. \quad (3)$$

The transit time (δ) taken by a voltage wave propagates along a single transmission line is given by

$$\delta = \frac{l\sqrt{\varepsilon_r}}{c} \text{ [s]}, \quad (4)$$

where l is the length of the transmission line and c is speed of light in vacuum. In Fig. 1, for the pulse forming process, the left end of the first transmission line (T1) must be shorted while the right end of the second transmission line (T2) is open. It is necessary, therefore, to use an inductor of inductance L_s to charge the transmission lines.

Fig. 2 illustrates the temporal voltage distribution at the terminals of the load. Here, the switch is closed at t=2.5 ns. The transit time is assumed to be 2.5 ns to produce a voltage pulse of 5 ns pulse duration. When the two transmission lines are fully charged to V_s by a power supply, the switch is closed and the pulse forming process is initiated. That is, a step voltage of -V_s propagates along T1 toward the load. After a transit time δ, the step voltage of -V_s arrives at the load. At this time (t=5 ns), the voltage at the right end of T1 is decreased to zero from V_s. One portion of the step voltage is reflected back along T1 and the other portion is transmitted into T1. Reflection coefficient (Γ) and transmission coefficient (τ) at the load are given by

$$\Gamma = \frac{Z_l}{Z_l + 2Z_o}, \quad \tau = \frac{2\left(Z_l + Z_o\right)}{Z_l + 2Z_o}. \quad (5)$$

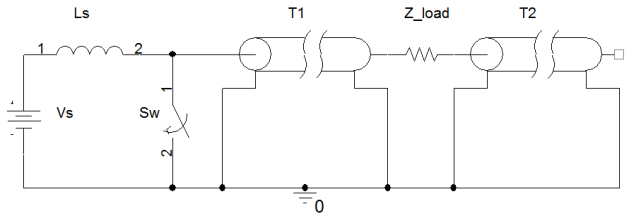

Fig. 1. Configuration of a single-stage Blumlein PFL

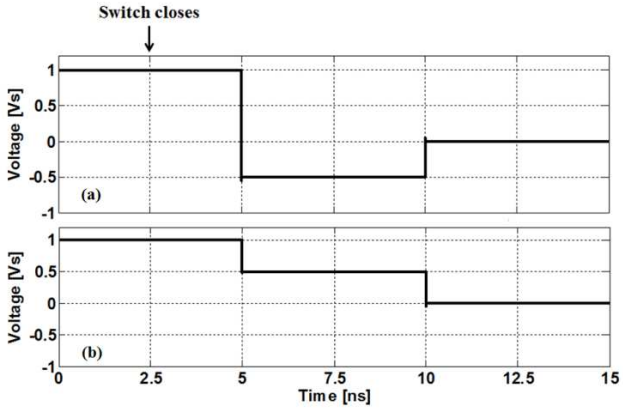

Fig. 2. Temporal voltage distribution on (a) left and (b) right terminals of the load.

To generate a square voltage pulse without any pulse reflections, the load impedance must equal twice the characteristic impedance of the transmission line. Substituting $Z_l = 2Z_o$ into Eq. (5), it is easy to obtain Γ=0.5 and τ=1.5. Thus, the voltage on T1 becomes -V_s/2 as a step voltage of -V_s/2 is reflected back to the switch. At the same time, a step voltage of -3V_s/2 is transmitted into the load and it is divided between the load and T2. That is, only a step voltage of -V_s/2 is launched into T2 and the voltage on T2 is changed to V_s/2 from V_s. As a result, the voltage across the load is V_s.

At t=7.5 ns, the reflected step voltage of -V_s/2 and the transmitted step voltage of -V_s/2 reach the left end of T1 and the right end of T2, respectively. A step voltage of V_s/2

is reflected along T1 toward the load because the reflection coefficient at the left end of T1 is -1. This step voltage arrives at the left load terminal at t=10 ns and the voltage there is changed to zero from -V_s/2. On the other hand, the transmitted step voltage of -V_s/2 is reflected from the open end of T2 without phase change and the voltage on the left end of T2 is decreased to zero from V_s/2 at t=10 ns.

After all forming processes, a square voltage pulse, whose amplitude is V_s and pulse duration is 2δ, is generated as shown in Fig. 3(a). In the case that the load impedance is not equal to twice the characteristic impedance of the transmission line ($Z_l \neq 2Z_o$), the main pulse is followed by several spurious reflections. As shown in Fig. 3(b), the amplitude of the main pulse under a condition of $Z_l > 2Z_o$ is relatively high compared to Fig. 3(a) and the polarity of reflections is always positive. On the other hand, the amplitude of the main pulse under a condition of $Z_l < 2Z_o$ is relatively low and the polarity of reflections alternates between positive and negative.

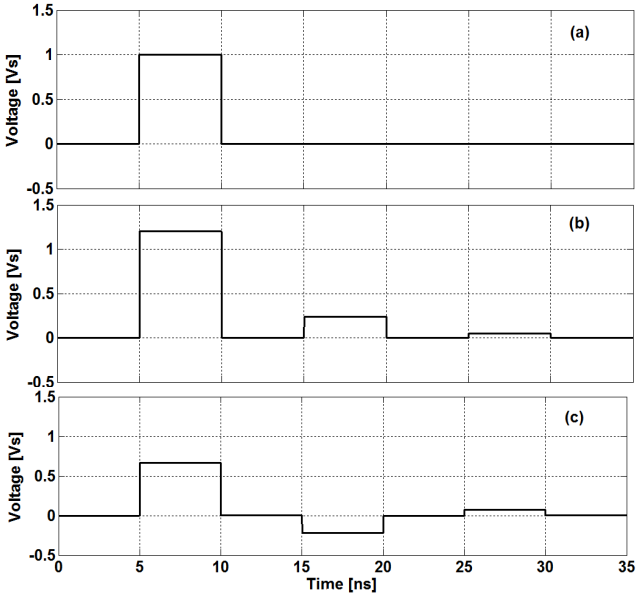

Fig. 3. Waveforms of output voltage pulses: (a) $Z_l = 2Z_o$; (b) $Z_l = 3Z_o$; (c) $Z_l = 0.5Z_o$

3. Blumlein Pulse Generators

Fig. 4 illustrates a cross-sectional view of the fabricated Blumlein pulse generator. The generator mainly consists of a pulse transformer, a spark gap switch, and a Blumlein PFL. All components are installed in a single cylindrical chamber. To ensure electrical insulation, the chamber is filled with transformer oil whose dielectric constant is 2.23. A charging circuit in Fig. 5 is connected to the pulse transformer. The stored energy of a ceramic capacitor with capacitance of 120 nF is discharged to the Blumlein PFL through the pulse transformer by closing a thyratron switch (E2V CX 1622 Model). The maximum charging voltage of the capacitor is 20 kV. A helical strip/wire type of air-cored pulse transformer is utilized to charge the Blumlein PFL up to more than 250 kV. The inductances of the pulse transformer are 9.8 μH and 5.92 mH at primary and secondary windings, respectively.

When the charging voltage of the Blumlein PFL reaches to a desired level, the spark gap switch closes automatically, thus initiating the operation of the Blumlein PFL. The breakdown voltage of the gap switch can be controlled by changing the gas pressure and the gap distance as well. The switch is filled with a mixture of SF_6 and N_2 gases. The gap distance between the electrodes is adjustable from 0 to 10 mm.

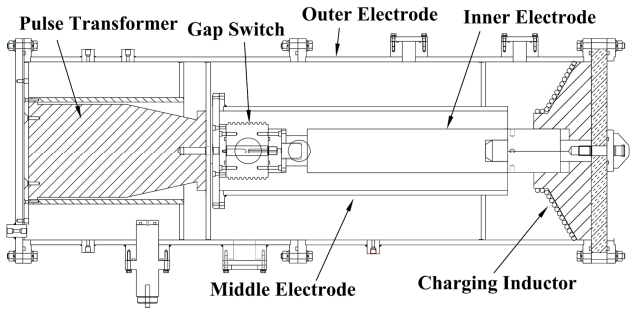

Fig. 4. Cross section of Blumlein pulse generator.

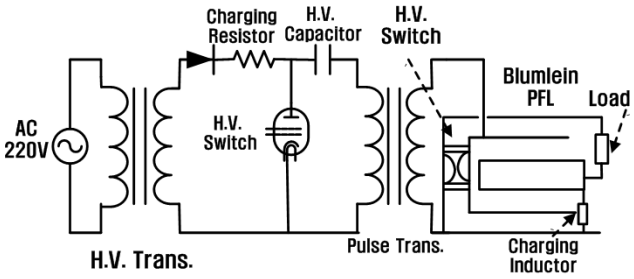

Fig. 5. Schematic diagram of the charging circuit.

As mentioned previously, a cylindrical type of Blumlein PFL is employed to form a high voltage pulse. In the Blumlein PFL, three cylindrical electrodes are concentrically placed to construct two coaxial transmission lines as shown in Fig. 4. The first transmission line is formed by middle and outer conductors and the second one is created by middle and inner conductors. Following are the dimensions of the Blumlein PFL. The radius of the inner conductor is 5 cm. Outer and inner radii of the middle conductor are 10 cm and 9 cm, respectively. The inner radius of the outer conductor is 20 cm. Note that the Blumlein chamber is filled with transformer oil; thus, $\mu_r = 1$ and $\varepsilon_r = 2.23$. From Eq. (3), the characteristic impedance can be calculated as Z_0=27.8 Ω for the first transmission line and Z_0=23.7 Ω for the second transmission line.

The use of a charging inductor is essential to connect the

inner conductor and the outer conductor while the Blumlein PFL is charged. The charging inductor is made of a wire of 1 mm diameter wound around half-conical MC nylon bobbin and its measured inductance is 1.2 mH.

4. PSpice simulation

Fig. 6 shows a schematic of PSPICE circuit to simulate the output pulse of the Blumlein pulse generator. Here, Tx indicates the pulse transformer with primary winding inductance of 9.8 μH and seconary winding inductance of 5.92 mH. Its coupling coefficient is 0.76. In the primary circuit of Tx, the capacitance of the charging capacitor (Cs) is 120 nF and the inductance of the inductor (Ls) is 2.5 μH. Two lossless transmission lines (T_middle_outer and T_middle_inner) are connected in parellel to model the Blumlein PFL. To measure the output pulse of the generator, a transmission line (T_line) is inserted between the Blumlein PFL and a purely resistive load of 50 Ω (Z_load). Its characteristic impedance and transit time are 50 Ω and 2.5 ns, respectively. The spark gap switch is modeled by SW and Lp denotes the stray inductance of the switch. The inductance of the charging inductor (Lc) is 1.2 mH. Cp is the stray capacitance associated with the charging inductor. Lt represents the inductance of the transition part between the Blumlein PFL and the charging inductor.

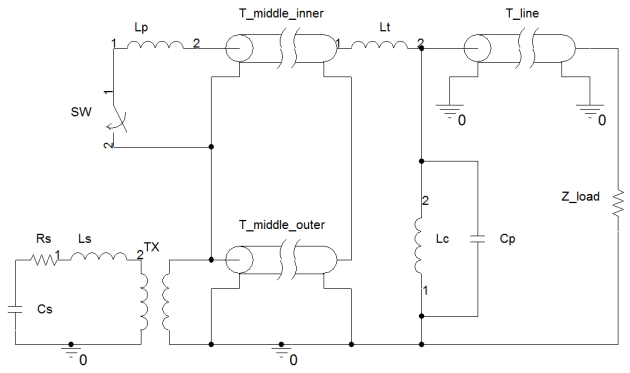

Fig. 6. PSPICE model of the Blumlein pulse generator

PSPICE simulations are performed to obtain the output voltage pulse from the Blumlein PFL for the following four cases. First of all, the output pulse is simulated under the condition that Lp, Cp and Lt are excluded from Fig. 6. The output pulse under this condition will be a reference pulse to examine effects of stray impedances. Fig. 7 illustrates the waveform of charging voltage on the transmission line as time changes. Here, the initial voltage of the charging capacitor (Cs) was set to be 16 kV. As can be seen, the charging voltage increases gradually and reaches to the maximum value (~250 kV) at t=1.7 μs. At this time, the switch is closed to discharge the transmission line. Fig. 8 shows the temporal development of the voltage pulse across the load after the switch is closed. A reflected pulse appears right after the main pulse unlike Fig. 3(b) and (c). Obviously, this reflected pulse is caused by the discrepancy between characteristic impedances of the two transmission lines. Note that the characteristic impedance of T_middle_outer is Z_0=27.8 Ω and the characteristic impedance of T_middle_inner is Z_0=23.7 Ω.

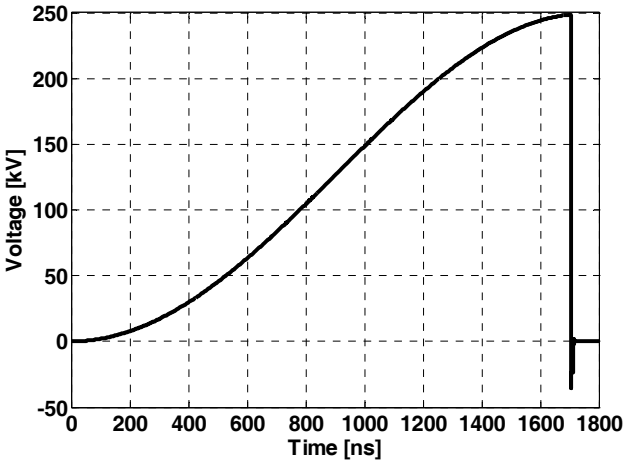

Fig. 7. Plot of charging voltage versus time

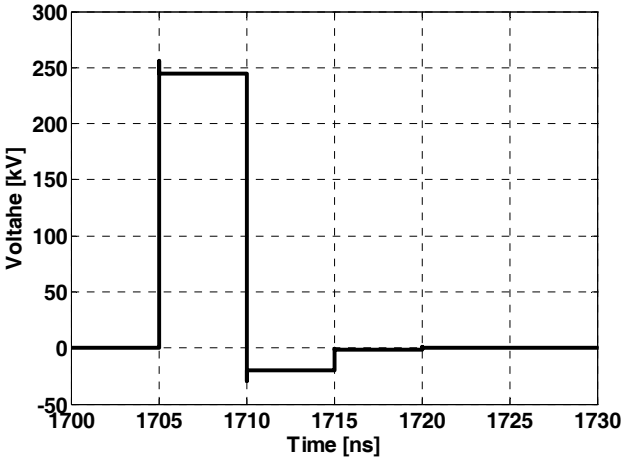

Fig. 8. Temporal development of the voltage pulse across the load without effects of stray inductance and capacitance

In the second case, only Lp is included in the simulation to examine its effects on the output pulse. The inductance of the spark channel depends on various factors such as operating gas pressure, interelectrode distance and applied voltage [9]. This implies that it is extremely difficult to obtain Lp analytically. It is assumed, therefore, that Lp is between 10 nH and 70 nH. Fig. 9 depicts simulation results obtained for four different values of stray inductance. As can be observed, Lp has a significant effect of distorting the pulse waveform. That is, the rise time and the pulse duration become longer as Lp increases. In addition, the peak voltage of the pulse decreases and reflected signals

appears with a relatively longer period after the main pulse.

In the third case, Cp as well as Lp is considered in the simulation. Cp is the sum of two capacitances; one is the turn-to-turn capacitance of the winding of the charging inductor and the other is the capacitance between the outer conductor and the winding. It is also difficult to analytically find the both capacitances due to the nonuniform structure of the charging inductor. It was revealed from numerous preliminary simulations that the capacitances ranging from 10 pF to 80 pF had meaningful effects on the waveform of the output pulse. Fig. 10 shows typical waveforms of the output pulse obtained with three different capacitances of 20 pF, 40 pF, and 60 pF. Here, Lp is 50 nH. As can be seen, the pulse waveform is affected by the change of the capacitance in such a way that the magnitude of the main pulse decreases but that of reflected pulses increases as the capacitance increases.

In the last case, the output pulse is simulated with all stray impedances included in Fig. 6. To verify simulation

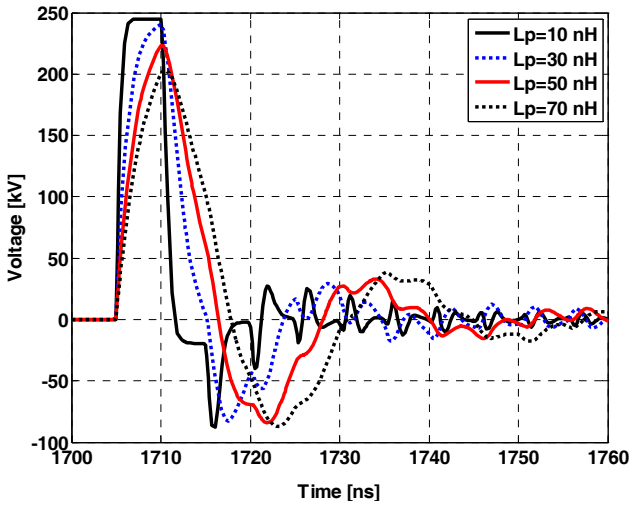

Fig. 9. Effects of stray switch inductance on waveforms of the voltage pulse across the load when Cp=0 and Lt=0.

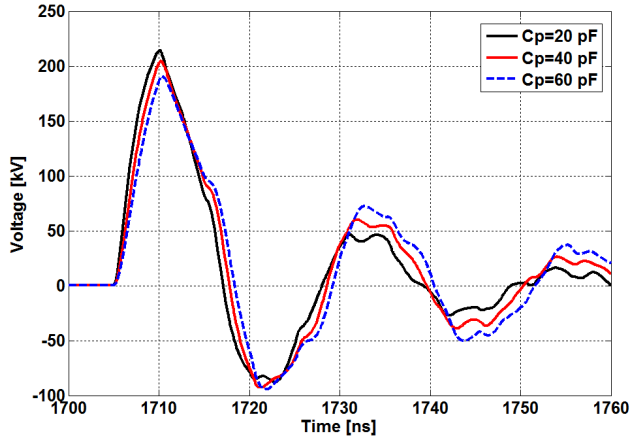

Fig. 10. Effects of stray capacitance on the waveform of the voltage pulse across the load when Lp=50 nH.

results, a simulated pulse waveform is compared to the actual pulse waveform obtained in the experiment. Fig. 11 illustrates an example of comparing the two waveforms. In the simulation, Lp=50 nH, Cp=40 pF, and Lt=40 nH. Overall, the simulated waveform shows an agreement with the actual waveform in terms of the amplitude and pulse duration of the main pulse. However, some discrepancy can be seen between the two waveforms after the main pulse.

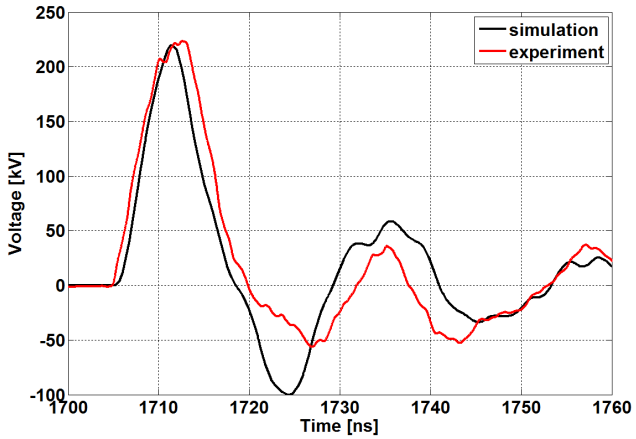

Fig. 11. Comparison of waveforms obtained in simulation and experiment.

5. Conclusion

A high voltage nanosecond pulse generator has been developed based on a cylindrical type of Blumlein PFL. PSPICE simulations have been performed to analyze the characteristics of the output pulse. Two transmission lines, a spark gap switch, a charging inductor, and a load are employed to model the Blumlein PFL. To examine the effects of stray inductance and capacitance on the output pulse, an inductor and a capacitor are connected in parallel to the switch and the charging inductor, respectively. According to the simulation results, the pulse waveform is significantly affected mainly by the stray inductance of the switch. Overall, the pulse waveform obtained in the simulation is in agreement with the experimental result. It is observed, however, that some discrepancies exist between simulated and actual waveforms. These are probably caused by transition sections of non-uniform characteristic impedance between the pulse transformer and the Blumlein PFL.

To improve the quality of the output pulse in terms of rise time and pulse duration, the stay inductance of the switch should be as small as possible. Therefore, it may be necessary to re-design the switch in the future. As an alternative, a peaking switch may be utilized to sharpen the waveform, thereby decreasing the rise time.

References

[1] A. D. Blumlein, "Improvements in or relating to apparatus for generating electrical impulses," GB Patent 589 127, 1947.

[2] P. W. Smith, *Transient Electronics - Pulsed Circuit Technology*, John Wiley & Sons, 2002.

[3] S. T Pai and Qi Zhang, *Introduction to High Power Pulse Technology*, World Scientific, Singapore, 1995.

[4] F. Davanloo, C. B. Collins, and F. J. Agee, "High power repetitive stacked Blumlein pulsers commutated by a single switch element," *IEEE Trans. Plasma Sci.*, Vol. 26, No. 5, pp. 1463-1475, Oct. 1998.

[5] V. P. Singal and B. S. Narayan, "Development of a Blumlein based on helical line storage elements," *Rev. Sci. Instrum.*, Vol. 72, No. 3, pp. 1862-1868, Mar. 2001.

[6] A. V. Martinez and V. Aboites, "High-efficiency low-pressure Blumlein nitrogen laser," *IEEE J. Quantum Electron.*, Vol. 29, No. 8, pp. 2364-2370, Aug. 1993.

[7] J. F. Kolb, S. Kono, and K. H. Schoenbach, "Nanosecond pulsed electric field generators for the study of subcellular effects," *Bioelectromagnetics*, Vol. 27, No. 3, pp. 172-187, 2006.

[8] J. Liu, Y. Yin, B. Ge, X. Cheng, J. Feng, J. Zhang, and X. Wang, "A compact high power pulsed modulator based on spiral Blumlein line", *Rev. Sci. Instrum*. Vol. 78, pp. 103302-1-103302-5, 2007.

[9] J. M. Lehr, C. E. Baum, and W. D. Prather and R. J. Torres, *Ultra-Wideband, Short-Pulse Electromagnetics 4*, Kluwer Academic/Plenum Publishers, pp. 11-20, 1999.

[10] G. Grandi, M. K. Kazimierczuk, A. Massarini, and U. Reggiani, "Stray Capacitances of Single-Layer Solenoid Air-Core Inductors", *IEEE Trans. Indus. Applications*, Vol. 35, No. 5, pp. 1162-1168, Sep. 1999

Young-Su Roh He received his B.S. and M.S. degrees in Electrical Engineering from Seoul National University in 1984 and 1986, respectively. He received a Ph.D. degree in Applied Science from the University of California, Davis in 2001. From 1988 to 1996, he worked at the Korea Electricity Research Institute. He is currently an Associate Professor at the Department of Electrical Engineering at Soongsil University. His research interests include plasma physics, nuclear fusion, and electrical discharges.

Yun-Sik Jin He received his B.S. and M.S. degrees in Nuclear Engineering from Seoul National University in 1986 and 1990, respectively. He received a Ph.D. degree in Plasma Science from the Nagasaki University 1999. From 1990 to present, he has been working at the Korea Electricity Research Institute (KERI). He is currently a team leader of pulsed power application at the Department of Electric Propulsion at KERI. His research interests include pulsed power generation & application, plasma application, and electrical discharges.